OPEN ACCESS

University of BRISTOL

Peer reviewed version

License (if available):
Unspecified

Link to published version (if available):
10.1021/acs.est.5b01190

Link to publication record in Explore Bristol Research
PDF-document

Article

Source apportionment of PAHs in Central European soils with compound-specific triple isotopes (#13C, #14C & #2H)

Carme Bosch, August Andersson, Martin Kruså, Cecilia Bandh, Ivana Hovorkova, Jana Klánová,
Timothy David James Knowles, Richard Pancost, Richard Peter Evershed, and Örjan Gustafsson

Just Accepted

1

2

3

4　**Source apportionment of PAHs in Central European soils with compound-**

5　**specific triple isotopes (δ^{13}C, Δ^{14}C & δ^2H)**

6

7

8　*Carme Bosch[1], August Andersson[1], Martin Kruså[1], Cecilia Bandh[1], Ivana Hovorková[2], Jana*

9　*Klánová[2], Tim Knowles[3], Richard D. Pancost[3], Richard P. Evershed[3] and Örjan Gustafsson[1,*]*

10

11　[1] Department of Environmental Science and Analytical Chemistry (ACES), and the Bolin Centre for Climate

12　Research, Stockholm University, 10691 Stockholm, Sweden

13　[2] Research Centre for Toxic Compounds in the Environment (RECETOX), Masaryk University, Kamenice

14　753/5, 62500 Brno, Czech Republic

15　[3] School of Chemistry, University of Bristol, Bristol BS8 1TS, Avon, England

16　*Corresponding author:

17　Örjan Gustafsson

18　Department of Environmental Science and Analytical Chemistry, Stockholm University

19　106 91 Stockholm, Sweden

20　Phone: +46 8 674 7317

21　Fax: +46 8 674 76 38

22　E-mail: orjan.gustafsson@aces.su.se

1

23 **ABSTRACT**

24 This paper reports the first study applying a triple-isotope approach for source apportionment

25 of polycyclic aromatic hydrocarbons (PAHs). The $^{13}C/^{12}C$, $^{14}C/^{12}C$ and $^2H/^1H$ isotope ratios of

26 PAHs were determined in forest soils from mountainous areas of the Czech Republic,

27 European Union. Statistical modeling applying a Bayesian Markov Chain Monte Carlo

28 (MCMC) framework to the environmental triple isotope PAH data and an end-member PAH

29 isotope database allowed comprehensive accounting of uncertainties and quantitative

30 constraints on the PAH sources between biomass combustion, liquid fossil fuel combustion,

31 and coal combustion at low and high temperatures. The results suggest that PAHs in this

32 central European region had a clear predominance of coal combustion sources ($75 \pm 6\%$;

33 uncertainties represent 1 SD), mainly coal pyrolysis at low temperature (~650 ºC) ($61 \pm 8\%$).

34 Combustion of liquid fossil fuels and biomass represented $16 \pm 3\%$ and $9 \pm 3\%$ of the total

35 PAH burden (ΣPAH_{14}), respectively. Although some soils were located close to potential

36 PAH point sources, the source distribution was within a narrow range throughout the region.

37 These observation-based top-down constraints on sources of environmental PAHs provides a

38 reference for both improved bottom-up emission inventories and guidance for efforts to

39 mitigate PAH emissions.

40 Keywords: Bayesian statistics, polycyclic aromatic hydrocarbons, coal combustion,

41 radiocarbon, stable carbon isotope, stable hydrogen isotope

42

43

44

45

46   **INTRODUCTION**

47   Polycyclic aromatic hydrocarbons (PAHs) are ubiquitous, predominantly anthropogenic,

48   organic molecules of environmental concern due to the mutagenic and carcinogenic properties

49   of some congeners (e. g., benzo[a]pyrene)[1]. Therefore, owing to their toxicity, they can pose a

50   threat to humans and the environment. Although PAHs are present in uncombusted petroleum

51   (i.e., petrogenic PAHs), the most important sources of PAHs in the environment are from the

52   incomplete combustion of biomass (e.g., wood) and fossil fuels (e.g., petroleum and coal)

53   (i.e., pyrogenic PAHs)[2,3]. In addition to their own negative effects, PAHs have also been

54   extensively used as molecular tracers of combustion-related airborne particles[3,4], which cause

55   numerous human health problems (e.g., lung cancer, respiratory and heart diseases)[5,6]. Among

56   atmospheric contaminants, PAHs account for most (35-82%) of the total mutagenic activity of

57   airborne particles[7] and hence, a reduction of PAH emissions is essential to improve air

58   quality.

59   Potential sources of airborne PAHs are vehicle exhaust, power generation, residential

60   heating/cooking, abrasion of tires and asphalt surfaces, waste incineration, and industrial

61   processes. A better understanding of PAH sources is essential to mitigate air pollution, but

62   unfortunately the relative contributions of different sources to PAHs are still poorly

63   understood. A variety of techniques to apportion sources of PAHs exist in the literature, based

64   on either molecular or isotopic compositions[3]. For instance, numerous studies have used

65   diagnostic ratios of PAH concentrations, usually isomeric ratios, to infer PAH sources[3,8,9].

66   However, the molecular composition of PAHs is affected by differential atmospheric removal

67   and transformation processes[9-11]. Furthermore, these isomeric ratios are not source specific

68   and show considerable intrasource variability[9]. The intrinsic carbon isotope composition of an

69   individual PAH molecule is a more conservative source tracer[12-15]. Although δ^{13}C analysis on

70   individual PAHs is a well-established technique[12,16,17], combining both compound-specific

71   stable isotope and (natural abundance) radiocarbon analyses (CSIA and CSRA, respectively)

72   offers a potentially far more powerful tool for quantitatively determining the sources of

73   contaminants in the environment. In the literature, combined compound-specific $\delta^{13}C$ and

74    $\Delta^{14}C$ measurements have been applied to apportion PAH sources in sediments[13,14], soils[18] and

75   air[15,19-22]. Introducing more isotope systems would naturally offer further improvements in

76   PAH source constraining capacity. As with any mass-balance approach the number of sources

77   that can be differentiated by N markers is N+1. Thus, the advantage of triple-isotope analysis

78   is that we can resolve four sources, rather than two (one marker) or three (two markers). Sun

79   and collaborators[23] reported the potential use of the stable hydrogen isotope in combination

80   with carbon isotopes for source apportionment of PAHs, but very few δ^2H-PAH

81   measurements in both emissions and ambient samples have been published to date. The only

82   δ^2H determinations performed in ambient emissions was limited to naphthalene, the simplest

83   PAH, from emissions of a combustion process in an alumina refinery[24]. Combining both

84   stable carbon and radiocarbon isotopes, with the hydrogen isotope analyses represents a

85   promising approach for elucidating sources of PAHs.

86   The aim of the present study is to demonstrate the triple-isotope approach ($\delta^{13}C$, $\Delta^{14}C$, δ^2H)

87   for the source apportionment of different PAHs by application to forest soils from the Czech

88   Republic. The Czech Republic is considered one of the most industrially-developed countries

89   among the new member states of the European Union and is used here as a representative for

90   Central Europe. The reason for studying the soil compartment is that PAHs in soil reflect a

91   longer-term input of pollutants compared to airborne concentrations. To the best of our

92   knowledge, by analyzing simultaneously three isotopes (stable carbon and hydrogen, and

93   radiocarbon), this study represents the first compound-specific application for source

94   apportionment using a triple-isotope approach.

95   **EXPERIMENTAL SECTION**

96 **Study Area.** Ten forest soil samples from mountainous sites within Czech Republic were

97 collected during September 2009 (Figure 1, Table 1). These mountain soils, which have been

98 repeatedly studied since 1995[25], mainly reflect atmospheric transport and deposition. Three

99 samples (#1, #2 and #3) were collected in the north-western part of the country. This border

100 region shared by Germany, Poland and Czech Republic and known as the "black triangle", is

101 characterized by extremely high levels of pollutant emissions[26]. Sample #1 was taken from

102 the Krušné Mts., relatively close to the town Litvínov, site of the largest oil refinery in the

103 Czech Republic. Three more samples (#4, #5 and #6) were collected in the Moravian Region

104 (NE Czech Republic). Two of them (#5 and #6) in the Beskydy Mts., located at the border

105 with Slovakia and adjacent to the industrial centers of Valasske Mezirici and Ostrava, which

106 contain a coal tar refinery (DEZA Corporation), a black carbon production plant (CABOT

107 CS) and seven hard coal mines (OKD Corp.). Sample #7 was collected near the observatory

108 of Košetice, a regional background station for international and national air monitoring

109 programmes. Samples #8, #9 and #10 were forest soils from the Bohemian Region (SW

110 Czech Republic), the Czech Bavarian forest. Spruce trees were the main vegetation type

111 found in all sampling sites. Details on soil sampling are described in the supplementary

112 material.

113 **Quantification of PAHs.** Analyses of PAHs were performed at the Research Centre for

114 Toxic Compounds in the Environment (RECETOX), Brno, Czech Republic. Briefly, an

115 aliquot of ca. 10 g dry soil was extracted using automated warm Soxhlet extraction with

116 dichloromethane (DCM). The extract was cleaned-up using activated silica flash column

117 chromatography and analytes eluted with DCM. The eluate was concentrated using a stream

118 of nitrogen in a concentrator unit, and transferred into a mini vial. Before injection, an internal

119 standard of terphenyl was added. Samples were analyzed by a 6890N GC (Agilent, USA)

120 capillary gas chromatography coupled to a mass spectrometer 5973N MS (Agilent, USA)

121 using electronic ionization (70 eV). PAHs were analyzed by selective ion recording (SIR).

122 Further details on sample extraction, clean-up, instrumental analysis and quality control

123 procedures are included in the supplementary material.

124 **Extraction of PAHs for Isotope Analysis.** Sample extraction for the isotope analysis was

125 performed at RECETOX, Brno, Czech Republic. Based on the concentrations found in the

126 individual soil samples in the previous step, the soil sample size needed to provide a sufficient

127 quantity of selected PAHs was determined. It varied between 500 and 1500 g of soil among

128 the top soil samples. Soxhlet-extracted samples with DCM were pre-cleaned using large

129 volume silica gel columns and concentrated. As the mountain forest soils contain large

130 amounts of organic material, additional clean-up was needed. Gel-permeation

131 chromatography was applied to remove high molecular weight compounds from the samples.

132 Samples were concentrated to a final volume of 1 ml for further isotope analyses. Further

133 information on these clean-up procedures is provided in the supplementary material. It has

134 been showed and reported that these purification procedures do not affect the original

135 molecular isotopic signatures. Results from studies on isotope fractionation during

136 purification procedures are included in the supplementary material.

137 **Isolation of PAHs for Radiocarbon Analysis.** Isolation of PAHs from soil extracts was

138 carried out at Stockholm University as previously described[14,27,28]. Extracts were repeatedly

139 injected onto a preparative capillary gas chromatography (pcGC) system programmed to trap

140 selected PAHs[14,29,30]. The pcGC system consisted of a gas chromatograph coupled to a flame

141 ionization detector 6890N GC (Agilent, Palo Alto, USA) and an autoinjector (7683A,

142 Agilent) integrated with a Gerstel cooled injection system (CIS), a zero-dead volume effluent

143 splitter and a Gerstel preparative trapping device. Since the abundance of the target PAH

144 compounds present in these soil samples was quite low relative to the requirements for ^{14}C

145 measurements (~20-100 µg), individual PAHs were pooled and trapped as follows: 1.

146   Phenanthrene (PHEN) + anthracene (ANTH); 2: fluoranthene (FLU) + pyrene (PYR); 3:

147   benz[a]anthracene (BaA) + triphenylene (TP) + chrysene (CHRY); 4: benzo[b]fluoranthene

148   (BbF) + benzo[j]fluoranthene (BjF) + benzo[k]fluoranthene (BkF); 5: benzo[e]pyrene (BeP) +

149   benzo[a]pyrene (BaP); 6: indeno[1,2,3-cd]pyrene (IcdP) + benzo[ghi]perylene (BghiP).

150   Additional details about chromatographic conditions and trapping procedures are included in

151   the Supporting Information.

152   **Analysis of Stable Carbon and Hydrogen Isotopes.** δ^{13}C and δ^2H analyses of soil extracts

153   were performed at The University of Bristol, UK. The δ^{13}C and δ^2H isotope ratio

154   determinations were performed by gas chromatography-isotope ratio mass spectrometry (GC-

155   IRMS). δ^{13}C analyses were performed using a ThermoQuest Finnigan DeltaPlusXL IRMS

156   coupled to an Agilent 6890 GC *via* a ThermoQuest Finnigan GC Combustion III interface.

157   δ^2H determinations were performed using a Thermo DeltaVPlus IRMS coupled to a Trace GC

158   *via* a GC Isolink and ConfloIV interface. For both δ^{13}C and δ^2H analyses, chromatographic

159   peaks were integrated in groups using the same 'chromatographic windows' described above

160   corresponding to those compounds which were isolated by pcGC, so as to accurately

161   represent the content of the samples analyzed by accelerator mass spectrometry (AMS). The

162   reported isotopic results, expressed in the per mil deviation (‰) of the isotope ratio from the

163   standards Peedee belemnite (PDB) and Vienna Standard Mean Ocean Water (VSMOW) for C

164   and H, respectively, represent the arithmetic means of triplicate analyses. Further information

165   on the instrumental analysis and quality procedures is provided in the supplementary material.

166   **Analysis of Radiocarbon.** The extracts for ^{14}C analysis were shipped to the US National

167   Ocean Sciences Accelerator Mass Spectrometry (NOSAMS) facility (Woods Hole, MA,

168   USA). The pcGC isolates were first purified, then combusted at 850 ºC for its conversion to

169   carbon dioxide and finally reduced to graphite. Targets of graphite were analyzed for ^{14}C by

170   AMS according to standard procedures[30-32]. All ^{14}C determinations are expressed as the per

171   mil (‰) deviation from NBS oxalic acid I. Further details about the ^{14}C analysis are included

172   in the Supplementary Information.

173   **Bayesian Markov Chain Monte Carlo method for source apportionment.** The three-

174   dimensional isotope signatures of the different PAHs were used in an isotopic mass balance

175   source apportionment model to differentiate four main sources: biomass, liquid fossil (e.g.,

176   petroleum and oil), low temperature (~650 ºC) coal combustion and high temperature (~900

177   ºC)   coal   combustion,   largely   following   our   earlier   dual-isotope   (three   source)

178   approaches[15,33,34]. The current study's four sources were selected based on two criteria: 1)

179   they encompass the majority of PAHs emitted in this region[35], 2) they are differentiable by

180   means of $\delta^{13}C$, $\Delta^{14}C$ and δ^2H isotopic signatures. In particular, we note that PAHs emitted

181   from high temperature coal combustion are more depleted in ^{13}C while more enriched in ^{2}H,

182   compared to coal combustion at lower temperatures[17].

183   The source-specific isotope values (end members) were collected from the literature, and are

184   summarized in Table S1. These end members are associated with significant variability and

185   uncertainties, especially in the δ^2H dimension. Such variability has recently been shown to

186   affect not only the precision of the source apportionment calculations, but also the estimated

187   central values (e.g., mean and median) of the source fractions[33]. To account for this variability

188   a Bayesian Markov Chain Monte Carlo (MCMC) approach was implemented[36], in which the

189   end member distributions are modelled as normal distributions with mean and standard

190   deviation defined by the literature values. The source-specific isotope values used in the

191   present study are listed in Table 2 and its calculation is detailed in the Supporting

192   Information. The MCMC approach effectively samples the 4-dimensional fractional source

193   space while satisfying the mass-balance criterion and accounting for the end member

194   variability. The result of the Bayesian approach is a probability density function (pdf) of the

195   relative source contribution for each source (Figure 3A). From this pdf the statistical

196   parameters of interest (e.g., mean, median, standard deviation or confidence intervals) may be

197   computed. The MCMC computations were run using an in-house written MATLAB version

198   2014a (The MathWorks, Natick, MA, USA) script, with 200,000 iterations, a burn-in (initial

199   search phase) of 10,000 and a data thinning of 10. The details of the Bayesian calculation is

200   published elsewhere[34] and the MATLAB script is presented in the present paper's Supporting

201   Information.

202   **RESULTS AND DISCUSSION**

203   **PAH Concentrations and Composition.** The PAHs input to mountain soils is mainly

204   through dry or wet deposition of aerosol particles or residues of vegetative litter, and by

205   processes of air-soil partitioning[37,38]. Forest soils are usually rich in organic matter, which

206   favors the accumulation of PAHs. The content of PAHs (sum of 14 PAHs) in the central

207   European forest soils ranged from 0.53 to 9.1 $\mu g \cdot g^{-1}$ (4.3 ± 2.8 $\mu g \cdot g^{-1}$, $\mu \pm \sigma$)(Table 1). These

208   concentrations were in agreement with previously reported concentrations at the same

209   sampling sites[25,39] (1.7-8.2 $\mu g \cdot g^{-1}$). As was expected from their proximity to emission sources,

210   the highest PAH loadings were observed at both northwestern (7.4 and 5.5 $\mu g \cdot g^{-1}$ for #1 and

211   #2 respectively) and eastern border regions (9.1 and 5.9 $\mu g \cdot g^{-1}$ for #5 and #6, respectively).

212   The lowest concentrations were found at Mt. Sumava, close to the border region shared with

213   Germany-Czech Republic-Austria (#9, 0.53 $\mu g \cdot g^{-1}$) and at the regional site of Kosetice (#7,

214   0.87 $\mu g \cdot g^{-1}$). All samples, except for #9, had a PAH content slightly higher than reported for

215   other remote/forest sites in Europe, such as in the Pyrenees[40] (0.77 $\mu g \cdot g^{-1}$), Alps[41] (1.3 ± 0.6

216    $\mu g \cdot g^{-1}$) and Tatras[41] (1.6 ± 0.4 $\mu g \cdot g^{-1}$). However, these border mountain soils may be also

217   affected by long range transport contamination coming from Poland, Germany, Slovakia or

218   Austria besides Czech Republic[42].

219   Relative PAH concentrations (Diagnostic Ratios, DR) are typically used for conventional

220   semiquantitative source apportionment through the comparison of the ambient ratios with

221   specific PAH source signatures. However, PAHs are affected by different atmospheric

222   processes and therefore the relative proportions of the PAH species are not conserved between

223   the emission source and the receptor site[10]. It is known that ANTH, BaA and BaP are

224   photochemically less stable in the atmosphere than PHEN, CHRY and BeP[43,44]. In the present

225   study, DRs were used to assess the extent of photochemical degradation of the studied

226   samples. Microbial degradation of PAHs that may change their isomer composition in

227   background surface soils is deemed unlikely to have a substantial effect on the source

228   apportionment results, considering the limited degradation observed in soils with high content

229   of organic matter affected by diffuse PAH pollution[45]. The BaA/(BaA+CHRY) and

230   BaP/(BeP+BaP) ratios ranged from 0.09 to 0.26 and from 0.13 to 0.44, respectively, and

231   correlate positively (R^2 = 0.90) (Table S2). Samples #1, #6 and #7 showed the largest

232   observed DRs (BaA/(BaP+BeP)>0.40 and BaA/(BaA+CHRY)>0.26, Table S2), indicating

233   that PAHs had been transported the shortest distance from the source. In contrast sample #10

234   presented the lowest ratios, thus the largest distance to the source.

235

236   **Carbon Isotope Composition of PAHs in Soils.** Compound-specific stable carbon isotope is

237   used to apportion sources. Polycyclic aromatic hydrocarbon (PAH) extracts from all samples

238   were analyzed for their stable carbon isotope composition (δ^{13}C). The δ^{13}C values ranged

239   between -25.3‰ and -23.0‰ (-24.0 ± 0.1‰, μ±σ) (Table 1 and Table S3). No substantial

240   variation was observed among sampling sites, which suggests a relatively homogenous

241   source. However, there was a consistent δ^{13}C variability between the different PAH

242   compounds, with the PAH group BaA + TP + CHRY (m/z 228) having the highest δ^{13}C

243   values (-23.4 ± 0.3‰) and the PAH group IcdP+BghiP (m/z 276) having the lowest δ^{13}C

244   values (-24.6 ± 0.3‰) (Figure 2A). This suggests that generation processes differed for the

245   different PAH molecules. During polyaromatization reactions, ^{13}C is preferentially lost during

246   C=C bond formation leading to a relative depletion in δ^{13}C values[46]. However, no positive

247   correlation was observed between molecular weight and δ^{13}C values. Overall the δ^{13}C values

248   of the PAHs in the present study were comparable to those observed in aerosols from Chinese

249   cities[47] (-26.3 to -24.4‰ in Chongqing and Hangzhou and -25.5 to -23.5‰ in Beijing) and

250   soils from a domestic coal-burning village near Glasgow, UK[48] (-25‰). δ^{13}C were, however,

251   generally more enriched in ^{13}C relative to ambient samples from other European countries

252   such as Sweden[15] (-28.9‰), Croatia[20] (-29.2‰) or Greece[20] (-29.0‰) and from archipelago

253   sediments in Stockholm, Sweden[14] (-27.0 to -24.8‰).

254   The radiocarbon content was determined for only those samples with sufficient analyte

255   concentrations (n = 7 sites). The determined Δ^{14}C values ranged between -960‰ and -768‰

256   (-892 ± 37‰) (Table 1 and Table S4). The radiocarbon composition exhibited very low

257   variability between different sampling sites and PAH compounds (Figure 2B), suggesting a

258   relatively homogenous source, which is consistent with the ^{13}C data. These highly depleted

259   ^{14}C signatures confirm that PAHs in these Czech forest soils are of a mainly fossil fuel origin.

260   Although the soil sample from Kosetice (#7) had slightly more modern carbon (less negative

261   signal) (-819‰, Table 1), those samples with the highest concentrations of PAHs had Δ^{14}C

262   values reflecting the largest fossil fuel contribution (#1, #2, #5 and #6 with Δ^{14}C ~ -942 and -

263   897‰, Table 1). Whereas the Czech border sites are mostly affected by long-range transport

264   of pollutants from industrial regions, more local impact is expected in Kosetice (#7). This

265   regional site belongs to an agricultural region with several small villages within 5-10 km in all

266   directions where wood is usually burned for domestic heating. PAHs in Czech Republic had

267   generally very high fossil contributions compared to PAHs from many other worldwide sites,

268   e.g., rural and background sites in Sweden[15,20] (-138 to +58‰ and -388 to -381‰,

269 respectively), western Balkans[22] (-568 to -288‰) and even a residential area in Tokyo[19] (-514

270 to -787‰).However, the Δ^{14}C-PAH values were similar to airborne PAHs from Croatia[20] (-

271 888‰), Greece[20] (-914‰), Alabama, US[21] (-980‰) and sediments from Stockholm,

272 Sweden[14] (-891 to -709‰).

273 **Hydrogen Isotope Composition of PAHs in Soils.** This is the first study complementing the

274 earlier reported dual compound-specific carbon isotope system of PAHs[14,15,22] with hydrogen

275 stable isotopic analyses. The PAH extracts exhibited δ^2H values between -263‰ and -53‰ (-

276 129 ± 44‰) (Table 1 and Table S5). In contrast to both carbon isotope systems (δ^{13}C and

277 Δ^{14}C), the deuterium system showed a higher variability among sampling sites. The western

278 border soil (#1) had a relatively much more ^{2}H-depleted value (-226‰) compared to #5 (δ^2H

279 ~ 135‰) or the remaining studied soils (#2, #6, #7, #8 and #10, δ^2H ~ -109‰). Other studies

280 have suggested that deuterium enrichment takes place simultaneously with ^{13}C depletion

281 during PAH generation[23]. However, in the present study no correlation was found between

282 PAH δ^{13}C and δ^2H values. Furthermore, no significant variability was observed between the

283 δ^2H values and the different PAHs (Figure 2A). Therefore, these data suggest that the

284 relatively more ^{2}H-depleted signature at site #1 reveals a PAH source different from the other

285 soils. To date, there have been no other studies on δ^2H values of PAHs in modern soils.

286 **Monte Carlo Simulations for Source Apportionment.** The compound-specific triple-

287 isotope approach allowed elucidation of up to four different sources. In the present study three

288 isotope signatures were analyzed, δ^{13}C, Δ^{14}C and δ^2H, for PAHs in forest soils from the Czech

289 Republic. The stable carbon isotope (δ^{13}C) is a priori informative for source apportionment

290 but it also has been shown that atmospheric photochemical processes can lead to ^{13}C

291 shifts[49,50]. However, O'Malley and collaborators evaluated the effects of evaporation,

292 photodecomposition and microbial degradation on the δ^{13}C values of individual PAHs and no

293 significant alterations were observed[12]. Furthermore, in the present study, no correlation was

12

294   found between the diagnostic ratios for photochemical degradation (BaA to BaA + CHRY

295   and BaP to BaP + BeP) and their respective $\delta^{13}C$ values (Figure S1). Based on this analysis,

296   carbon isotopic fractionation of PAHs during atmospheric transport was therefore likely

297   insignificant and $\delta^{13}C$ values were used to apportion PAH sources.

298   The natural abundance of radiocarbon ($\Delta^{14}C$) was utilized to differentiate between fossil fuel

299   (-1000‰) *versus* combustion of contemporary sources (+137.5 ± 21.9‰) for PAHs. Stable

300   carbon isotope ratio determinations of individual PAHs showed different $\delta^{13}C$ values for the

301   combustion of C_3 terrestrial vegetation[51-53] (e.g., wood, ~ -28.7‰) and liquid fossil fuels[23,52,54]

302   (e.g., gasoline, ~ -24.1‰, diesel, ~ -26.5‰). Regarding the individual PAHs derived from

303   coal combustion sources, $\delta^{13}C$ values have been shown to vary over a wide range by ca.

304   8‰[17,23,52,55-57] (-31 to -23‰) and overlapping with C_3 wood and liquid fossil fuel sources. The

305      $\delta^{13}C$ values of coal-derived PAHs are normally dictated by both the isotopic signature of the

306   parent fuels and the temperature of combustion. In general, PAHs derived from carbonization

307   processes at low temperatures (~650 ºC) have isotopic values similar to those of the parent

308   coals[17,52,58-60] (-25.4 to -21‰), because they are mainly primary devolatilisation products from

309   mild combustion processes[17]. Instead, $\delta^{13}C$ values of PAHs became lighter when the

310   temperature of carbonization is higher (~900 ºC) because they are then products of

311   condensation reactions, which result in a kinetic isotope effect with ^{12}C-^{12}C bonds forming

312   more easily than ^{13}C-^{12}C bonds[17,23,52,55] (-29.4 to -24.2‰).

313   In contrast to their $\delta^{13}C$ values, the δ^2H values of PAHs generated by coal, biomass and liquid

314   fuel pyrolysis differ substantially (e.g., liquid fossil fuels[23,53], -76 to -47‰; C_3 wood[53] ~ -

315   94‰; high coal pyrolysis[23], -81 to -65‰; bulk coals[58,60], -170 to -87‰; and bulk peat[61-63], -

316   240 to -79‰). However, only few source-specific δ^2H values have been reported in the

317   scientific literature to date. Therefore, in the future there is the need to better characterize the

318   hydrogen isotopic signature of primary sources. Although δ^2H literature values are currently

319   limited, the simultaneous use of $\delta^{13}C$, $\Delta^{14}C$ and δ^2H provide a greater differentiation and

320   allowed quantitatively to apportion the relative contribution of four different combustion

321   source classes to the PAH. Source-specific $\delta^{13}C$ and δ^2H values reported in literature are

322   summarized in the Supporting Information (Table S1).

323   The choice of sources to perform the Bayesian-based method (see Experimental Section) was

324   based on existing bottom-up emission inventories and past PAH fingerprinting studies

325   indicating the major sources of PAHs in the Czech Republic[35,64-66]. By combining the isotopic

326   signatures of sample data and primary PAH sources in two-dimensional plots (Figures

327   2A+B), the following four sources were chosen: combustion of liquid fuels, C_3 wood

328   combustion, as well as coal combustion at low (~650 ºC) and high (~900 ºC) temperatures.

329   The isotopic signatures used for the primary PAHs sources are detailed in Table 2.

330   Natural peat fires in the border mountainous Czech areas were a priori a potential source of

331   PAHs in Czech Republic. However, the present PAH-isotope data did not support this

332   hypothesis (Figure 2A+B). Furthermore, the soil from the northwestern part of the country

333   (#1) had a hydrogen stable-isotope composition which was more depleted in ^2H than the other

334   samples and moreover, did not match any of the primary sources explored for δ^2H values of

335   PAHs in the literature to date (Figure 2A+B). Shifts in the δ^2H values of organic molecules

336   have been observed as a result of many degradation processes with potentially quite large

337   enrichment factors[67]. However, such deuterium fractionation is generally accompanied with a

338   shift also in the $\delta^{13}C$ values, which was not observed in the case of sample #1. It is worth

339   noting here that the lack of reported source-specific data for the hydrogen isotope composition

340   makes it difficult to draw other interpretations of sample #1. As a result, sample #1 was not

341   considered for the Bayesian-based data analysis due to the inability to associate its δ^2H values

342   to either a primary source or a degradation process. Nevertheless, the results of the

343   radiocarbon analyses of site #1 enabled the calculation of the relative contributions of the

344   combined fossil fuel sources *versus* contemporary biomass using a simple isotopic mass

345   balance equation as described elsewhere[14] (Table 3 and Figure 3B).

346   The compound-specific isotope ratios for every site were combined with literature values for

347   source end members in a mass balance-based source-apportionment scheme. The variability

348   of the isotopic source signatures were accounted for within a Bayesian Markov Chain Monte

349   Carlo framework. Four probability density functions, one for every source, were obtained for

350   every group of PAHs and site (#2, #5, #6, #7, #8 and #10), as is shown at Figure 3A for the

351   group BbF+BjF+BkF and site#7. All samples showed a similar source pattern with the highest

352   contribution coming from the coal combustion at low temperature, ranging from 53 to 75%

353   (61±8%, Table 3 and Figure 3B). Practically equal contributions from liquid fossil fuels and

354   coal combustion at high temperature were also observed for all samples (16 ± 3% and 13 ±

355   2%, respectively). Biomass combustion was the least important source of PAHs in Czech

356   Republic soils, with contributions ranging between 5 to 16% (9 ± 3%). Only small differences

357   were observed between samples, but those soils with the highest PAH concentrations from the

358   northwestern (#1 and #2) and the eastern border (#5 and #6) regions had slightly higher coal-

359   related contributions (Figure 3B, high + low temperatures coal combustion ~ 74-85% and

360   biomass ~ < 9%). Correspondingly, soils from Kosetice and the southern region had slightly

361   higher biomass contributions (#7, #8 and #10, biomass ~ 10-16% and coal ~ 66-74%).

362   Although some soil sites were placed relatively close to potential PAH point sources and

363   showed higher PAH concentrations, the triple-isotope-based apportionment demonstrated that

364   the contribution from the four different source classes were rather homogeneous for

365   mountainous forest soils across the country. The low observed biomass contributions (9 ±

366   3%) in Czech background soils are similar to those observed in South Europe, such as in

367   background air from Croatia and Greece[20] (9% and 7%, respectively), but lower than those in

368   North Europe (i.e. Sweden[20], 50%)

369   Coal combustion at low and high temperatures may be associated to domestic and industrial

370   emissions, respectively. Additionally, combustion of fuels at low temperature has the

371   potential to result in higher PAH emissions than high-temperature combustion sources (i.e.

372   the lower is the combustion temperature, higher are the PAHs emission factors[4]). These high

373   emission factors might explain the high contribution coming from low-temperature coal

374   combustion sources in Czech Republic. However, the household coal usage represents only

375   the 3% of the total coal production in the Czech Republic[68]. Furthermore, the residential coal

376   burning represents one of the most toxic sources of PAHs due to both high emission rates and

377   proximity to population[35]. Emission inventories show a reduction of PAH emissions in recent

378   years in almost all European countries, being the residential sector the most important source

379   of PAHs nowadays[35]. In 2007, residential emissions (including fossil and non-fossil sources)

380   accounted for the 47.5% of the total PAH emissions in Europe[35]. The present study shows like

381   the residential sector in Czech Republic, in particular the residential coal burning, may be

382   more important than the European average. Taken together, PAHs in Czech soils are heavily

383   influenced by coal combustion practices (75%), mainly coming from household emissions

384   (61%).

385   The present study demonstrates firstly that triple isotope characterization of PAHs is possible

386   and secondly, that this information is useful for source characterization. However, the existing

387   literature on isotope characterization of PAHs is currently limited. We think and hope that the

388   current contribution may encourage researchers to expand the existing source database. Such

389   work should seek to both improve the statistics for the currently investigated sources, but also

390   expand the number of source categories in terms of their geographical prevalence.

391

392   **REFERENCES**

393   (1)   Agency for Toxic Substances and Disease Registry (ATSDR), **1995**. Toxicological

394   profile for polycyclic aromatic hydrocarbons (PAHs). Atlanta, GA: U.S. *Department of*

395   *Health and Human Services, Public Health Service.*

396   (2)   Gustafsson, Ö.; Buesseler, K. O.; Gschwend, P. M. Using ^{234}Th disequilibria to

397   estimate the vertical removal rates of polycyclic aromatic hydrocarbons from the surface

398   ocean. *Mar. Chem.* **1997**, 57, 11-23.

399   (3)   Lima, A. L .C.; Farrington, J. W.; Reddy, C. M. Combustion-derived polycyclic

400   aromatic hydrocarbons in the environment – a review. *Environ. Forensics* **2005**, *6*, 109-131.

401   (4)   Ravindra, K.; Sokhi, R.; Van Grieken, R. Atmospheric polycyclic aromatic

402   hydrocarbons: source attribution, emission factors and regulation. *Atmos. Environ*. **2008**, *42,*

403   2895-2921.

404   (5)   Beelen, R. *et al.* Effects of long-term exposure to air pollution on natural-cause

405   mortality: an analysis of 22 European cohorts within the multicentre ESCAPE project.

406   *Lancet***2014,** 383, 785-795.

407   (6)   WHO, 2014. Outdoor Air Pollution in the World Cities. World Health Organization,

408   Geneva, Switzerland. http://www.who.int/phe/health_topics/outdoorair/databases/en.

409   (7) Pedersen, D. U.; Durant, J. L.; Penman, B. W.; Crespi, C. L.; Hemond, H. F.; Lafleur, A.

410   L.; Cass, G. R. Human-cell mutagens in respirable airborne particles in the northeastern

411   United States. 1. Mutagenicity of fractionated samples. *Environ. Sci. Technol*. **2004,** *38,* 682-

412   689.

413   (8) Nam, J. J.; Thomas, G. O.; Jaward, F. M.; Steinnes, E.; Gustafsson, Ö.; Jones K. C. PAHs

414   in background soils from Western Europe: Influence of atmospheric deposition and soil

415   organic matter. *Chemosphere* **2008**, *70*, 1596-1602.

416   (9) Galarneau, E. Source specificity and atmospheric processing of airborne PAHs:

417   Implications for source apportionment. *Atmos. Environ.* **2008***, 42,* 8139-8149.

418   (10) Dvorská, A.; Lammel, G.; Klánová, J. Use of diagnostic ratios for studying source

419   apportionment and reactivity of ambient polycyclic aromatic hydrocarbons over Central

420   Europe. *Atmos. Environ.* **2011***, 45,* 420-427.

421   (11) Kim, D.; Kumfer, B. M.; Anastasio, C.; Kennedy, I. M.; Young, T. M. Environmental

422   aging of polycyclic aromatic hydrocarbons on soot and its effect on source identification.

423   *Chemosphere* **2009**, *76*, 1075-1081.

424   (12) O'Malley, V.; Abrajano, Jr. T.; Hellou, J. Determination of the $^{13}C/^{12}C$ ratios of

425   individual PAH from environmental samples: Can PAH sources be apportioned?. *Org.*

426   *Geochem.* **1994,** *21*, 809-822.

427   (13) Reddy, C. M.; Pearson, A.; Xu, L.; McNichol, A. P.; Benner, B. A.; Wise, S. A.; Klouda,

428   G. A.; Currie, L. A.; Eglinton, T. I. Radiocarbon as a tool to apportion the sources of

429   polycyclic aromatic hydrocarbons and black carbon in environmental samples. *Environ. Sci.*

430   *Technol.* **2002,** *36,* 1774-1782.

431   (14) Mandalakis, M.; Gustafsson, Ö.; Reddy, C. M.; Xu, L. Radiocarbon Apportionment of

432   Fossil versus Biofuel Combustion Sources of Polycyclic Aromatic Hydrocarbons in the

433   Stockholm Metropolitan Area. *Environ. Sci. Technol*. **2004**, *38*, 5344-5349.

434   (15) Sheesley, R. J.; Kruså, M.; Krecl, P.; Johansson, C.; Gustafsson, Ö. Source

435   apportionment of elevated wintertime PAHs by compound-specific radiocarbon analysis.

436   *Atmos. Chem. Phys*. **2009**, *9*, 3347-3356.

437   (16) McRae, C.; Snape, C. E.; Sun, C.; Fabbri, D.; Tartari, D.; Trombini, C.; Fallick, A. E.

438   Use of compound-specific stable isotope analysis to source anthropogenic natural gas-derived

439   polycyclic aromatic hydrocarbons in a lagoon sediment. *Environ. Sci. Technol.* **2000**, *34*,

440   4684-4686.

441   (17) McRae, C.; Sun, C.; Snape, C. E.; Fallick, A. E.; Taylor, D. δ^{13}C values of coal-derived

442   PAHs from different processes and their application for source apportionment. *Org.*

443   *Geochem.* **1999**, *30*, 881-889.

444   (18) Lichtfouse, E.; Budzinski, H.; Garrigues, H. P.; Eglinton, T. I. Ancient polycyclic

445   aromatic hydrocarbons in modern soils: ^{13}C, ^{14}C and biomarker evidence. *Org. Geochem.*

446   **1997**, *26*, 353-359.

447   (19) Kumata, H.; Uchida, M.; Sakuma, E.; Uchida, T.; Fujiwara, K.; Tsuzuki, M.; Yoneda,

448   M.; Shibata, Y. Compound class specific C-14 analysis of polycyclic aromatic hydrocarbons

449   associated with PM_{10} and $PM_{1.1}$ aerosols from residential areas of suburban Tokyo. *Environ.*

450   *Sci. Technol.* **2006**, *40*, 3474-3480.

451   (20) Mandalakis, M.; Gustafsson, Ö.; Alsberg, T.; Egebäck, A. L.; Reddy, C. M.; Xu, L.;

452   Klanova, J.; Holoubek, I.; Stephanou, E. G. Contribution of Biomass Burning to Atmospheric

453   Polycyclic Aromatic Hydrocarbons at Three European Background Sites. *Environ. Sci.*

454   *Technol.* **2005**, *39*, 2976-2982.

455   (21) Xu, L.; Zheng, M.; Ding, X.; Edgerton, E.; Reddy, C. M. Modern and fossil contributions

456   to polycyclic aromatic hydrocarbons in PM2.5 from North Birmingham, Alabama in the

457   southeastern U.S. *Environ. Sci. Technol.* **2012**, *46*, 1422-1429.

458   (22) Zencak, Z.; Klanova, J.; Holoubek, I; Gustafsson, Ö. Source apportionment of

459   atmospheric PAHs in the western Balkans by natural abundance radiocarbon analysis.

460   *Environ. Sci. Technol.* **2007**, *41*, 3850-3855.

461   (23) Sun, C.; Cooper, M.; Snape, C. E. Use of compound-specific δ^{13}C and δD stable isotope

462   measurements as an aid in the source apportionment of polyaromatic hydrocarbons. *Rapid*

463   *Commun. Mass Spectrom.* **2003**, *17*, 2611-2613.

464   (24) Vitzthum von Eckstaedt, C. D.; Grice, K.; Ioppolo-Armanios, M.; Jones, M. δ^{13}C and δD

465   of volatile organic compounds in an alumina industry stack emission. *Atmos. Environ.* **2011**,

466   *45*, 5477-5483.

467   (25) Kukucka, P.; Klanova, J.; Sanka, M.; Holoubek, I. Soil burdens of persistent organic

468   pollutants – Their levels, fate and risk. Part II. Are there any trends in PCDD/F levels in

469   mountain soils? *Environ. Pollut.* **2009**, *157*, 3255-3263.

470   (26) van Drooge, B. L.; Fernández, P.; Grimalt, J. O.; Stuchlík, E.; Torres García, C.J.;

471   Cuevas, E. Atmospheric polycyclic aromatic hydrocarbons in remote European and Atlantic

472   sites located above the boundary mixing layer. *Environ. Sci. Pollut. Res.* **2010**, *17*, 1207-1216.

473
474   (27) Mandalakis, M. and Ö. Gustafsson. Optimization of a preparative capillary gas

475   chromatography-mass spectrometry system for the isolation and harvesting of individual

476   polycyclic aromatic hydrocarbons. *J. Chromatogr. A.* **2003**, *996*, 163-172.

477   (28) Meinert, C. and W. Brack. Optimisation of trapping parameters in preparative capillary

478   gas chromatography for the application in effect-directed analysis. *Chemosphere* **2010**, *78*,

479   416-422.

480   (29) Eglinton, T. I.; Aluwihare, L. I.; Bauer, J. E.; Druffel, E. R. M.; McNichol, A. P. Gas

481   chromatographic isolation of individual compounds from complex matrices for radiocarbon

482   dating. *Environ. Sci. Technol.* **1996***, 68,* 5, 904-912.

20

483   (30) Zencak, Z.; Reddy, C. M.; Teuten, E. L.; Xu, L.; McNichol, A. P.; Gustafsson, Ö.

484   Evaluation of gas chromatographic isotope fractionation and process contamination by carbon

485   in compound-specific radiocarbon analysis. *Anal. Chem.* **2007**, *79*, 2042-2049.

486   (31) Pearson, A.; McNichol, A. P.; Schneider, R. J.; von Reden, K. F.; Zheng, Y. Microscale

487   AMS ^{14}C measurement at NOSAMS. *Radiocarbon* **1998,** *40*, 61-75.

488   (32) McNichol, A. P.; Gagnon, A. R.; Jones, G. A.; Osborne, E.A. Illumination of a Black-

489   Box - Analysis of Gas-Composition During Graphite Target Preparation. *Radiocarbon* **1992,**

490   *34*, 321-329.

491   (33) Andersson, A. A systematic examination of a random sampling strategy for source

492   apportionment calculations. *Sci. Total Environ.* **2011**, *412-413*, 232-238.

493   (34) Andersson, A.; Deng, J.; Du, K.; Zheng, M.; Yan, C.; Sköld, M.; Gustafsson, Ö.

494   Regionally-varying combustion sources of the January 2013 severe haze events over eastern

495   China. *Environ. Sci. Technol.* **2015**, *49*, 2038-2043.

496   (35) Shen, H.; Huang, Y.; Wang, R.; Zhu, D.; Li, W.; Shen, G.; Wang, B.; Zhang, Y.; Chen,

497   Y.; Lu, Y.; Chen, H.; Li, T.; Sun, K.; Li, B.; Liu, W.; Liu, J.; Tao, S. Global atmospheric

498   emissions of polycyclic aromatic hydrocarbons from 1960 to 2008 and future predictions.

499   *Environ. Sci. Technol*. **2013**, *47*, 6415-6424.

500   (36) Parnell, A. C., Inger, R., Bearhop, S., Jackson, A. L. Source apportionment using stable

501   isotopes: coping with too much variation. *PLOS one 5* **2010**, 1-5.

502   (37) Ribes, A., van Drooge, B. L., Dachs, J., Gustafsson, Ö., Grimalt, J. O. Influence of Soot

503   Carbon on the Soil-Air Partitioning of Polycyclic Aromatic Hydrocarbons. *Environ. Sci.*

504   *Technol.* **2003**, *37,* 2675-2680.

505   (38) Nam, J. J., Thomas, G. O., Jaward, F. M., Steinnes, E., Gustafsson, Ö., Jones, K. C.

506   PAHs in background soils from Western Europe: Influence of atmospheric deposition and soil

507   organic matter. *Chemosphere* **2008**, *70,* 1596-1602.

508   (39) Holoubek, I.; Dusek, L.; Sanka, M.; Hofman, J.; Cupr, P.; Jarkovsky, J.; Zbiral, J.;

509   Klanova, J. Soil burdens of persistent organic pollutants – Their levels, fate and risk. Part I.

510   Variation of concentration ranges according to different soil uses and locations. *Environ.*

511   *Pollut.* **2009**, *157,* 3207-3217.

512

513   (40) Grimalt, J. O.; van Drooge, B.; Ribes, A.; Fernández, P.; Appleby, P. Polycyclic aromatic

514   hydrocarbon composition in soils and sediments of high altitude lakes. *Environ. Pollut*. **2004**,

515   *131*, 13-24.

516   (41) Quiroz, R.; Grimalt, J. O.; Fernandez, P.; Camarero, L.; Catalan, J.; Stuchlik, E.; Thies,

517   H.; Nickus, U. Polycyclic aromatic hydrocarbons in soils from European high mountain areas.

518   *Water Air Soil Pollut.* **2011**, *215,* 655-666.

519   (42) Dvorska, A.; Lammel, G.; Klanova, J.; Holoubek, I. Košetice, Czech Republic – ten

520   years of air pollution monitoring and four years of evaluating the origin of persistent organic

521   pollutants. *Environ. Pollut.* **2008,** *156*, 403-408.

522   (43) Behymer, T. D.; Hites, R. A. Photolysis of polycyclic aromatic hydrocarbons adsorbed

523   on fly ash. *Environ. Sci. Technol.* **1988**, *22,* 1311-1319.

524   (44) Perraudin, E.; Budzinski, H.; Villenave, E. Kinetic study of the reactions of NO_2 with

525   polycyclic aromatic hydrocarbons adsorbed on silica particles. *Atmos. Environ.* **2005**, *39,*

526   6557-6567.

527   (45) Johnsen, A. R.; Karlson, U. Diffuse PAH contamination of surface soils: environmental

528   occurrence, bioavailability, and microbial degradation. *Appl. Microbiol. Biotechnol.* **2007**, *76,*

529   533-543.(46) Bird, M. I.; Ascough, P. L. Isotopes in pyrogenic carbon: A review. *Org.*

530   *Geochem.* **2012**, *42*, 1529-1539.

531   (47) Okuda, T.; Kumata, H.; Naraoka, H.; Takada, H. Origin of atmospheric polycyclic

532   aromatic hydrocarbons (PAHs) in Chinese cities solved by compound-specific stable carbon

533   isotopic analyses. *Org. Geochem.* **2002,** *33*, 1737-1745.

534   (48) McRae, C.; Sun, C.; McMillan, C. F.; Snape, C. E.; Fallick, A. E. Sourcing of fossil fuel-

535   derived PAH in the environment. *Polycyclic Aromatic Compd.* **2000**, *20*, 97.

536   (49) Aggarwal, S. G.; Kawamura, K. Molecular distributions and stable carbon isotopic

537   compositions of dicarboxylic acids and related compounds in aerosols from Sapporo, Japan:

538   Implications for photochemical aging during long-range atmospheric transport, *J. Geophys.*

539   *Res.-Atmos.* **2008**, *113*, D14301, doi:10.1029/2007JD009365.

540   (50) Pavuluri, C. M.; Kawamura, K. Evidence for 13-carbon enrichment in oxalic acid via

541   iron catalyzed photolysis in aqueous phase. *Geophys. Res. Lett.*, **2012**, *39,* L03802, doi:

542   10.1029/2011GL050398.

543   (51) O'Malley, V.; Burke, R.A.; Schlutzhauer, W.S. Using GC-MS/Combustion/IRMS to

544   determine the $^{13}C/^{12}C$ ratios of individual hydrocarbons produced from the combustion of

545   biomass materials – application to biomass burning. *Org. Geochem.* **1997,** *27*, 567-581.

546   (52) McRae, C.; Love, G. D.; Murray, I. P.; Snape, C. E.; Fallick, A. E. Potential of gas

547   chromatography isotope ratio mass spectrometry to source polycyclic aromatic hydrocarbon

548   emissions. *Anal. Commun.,* **1996**, *33*, 331-333.

549 (53) Vitzthum von Eckstaedt, C. D.; Grice, K.; Ioppolo-Armanios, M.; Kelly, D.; Gibberd, M.

550 Compound specific carbon and hydrogen stable isotope analyses of volatile organic

551 compounds in various emissions of combustion processes. *Chemosphere* **2012**, *78*, 1407-

552 1413.

553 (54) Okuda, T.; Kumata, H.; Zakaria, M.P.; Naraoka, H.; Ishiwatari, R.; Takada, H. Source

554 identification of Malaysian atmospheric polycyclic aromatic hydrocarbons nearby forest fires

555 using molecular and isotopic compositions. *Atmos. Environ.* **2002,** *36*, 611-618.

556 (55) McRae, C.; Snape, C. E.; Fallick, A. E. Variations in the stable ratios of specific aromatic

557 and aliphatic hydrocarbons from coal conversion processes. *Analyst* **1998***, 123,* 1519-1523.

558 (56) Chen, Y. J.; Cai, W. W.; Huang, G. P.; Li, J.; Zhang, G. Stable Carbon Isotope of Black

559 Carbon from Typical Emission Sources in China. *Environ. Sci.* **2012**, *33,* 673-678 (in

560 Chinese).

561 (57) Kawashima, H.; Haneishi, Y. Effects of combustion emissions from the Eurasian

562 continent in winter on seasonal $\delta^{13}C$ of elemental carbon in aerosols in Japan. *Atmos. Environ.*

563 **2012,** *46,* 568-579.

564 (58) Redding, C. E.; Schoell, M.; Monin, J. C.; Durand, B. Hydrogen and carbon isotopic

565 composition of coals and kerogens. *Phys. Chem. Earth* **1980**, *12*, 711-723.

566 (59) Gleason, J. D. and Kyser, T. K. Stable isotope compositions of gases and vegetation near

567 naturally burning coal. *Nature* **1984**, *307*, 254-257.

568 (60) Mastalerz, M. and A. Schimmelmann. Isotopically exchangeable organic hydrogen in

569 coal relates to thermal maturity and maceral composition. *Org. Geochem.* **2002***, 33,* 921-931.

24

570   (61) Jedrysek, M-O.; Skrzypek, G. Hydrogen, carbon and sulphur isotope ratios in peat: the

571   role of diagenessis and water regimes in reconstruction of past climates. *Environ. Chem. Lett.*

572   **2005**, *2Q*:179–183, doi: 10.1007/s10311-004-0093-4.

573   (62) Skrzypek, G.; Paul, D.; Wojtun, B. Stable isotope composition of plants and peat from

574   Arctic mire and geothermal area in Iceland. *Pol. Polar Res.* **2008**, *29 (4),* 365–376.

575   (63) Seki, O.; Meyers, P. A.; Kawamura, K.; Zheng, Y.; Zhou, W. Hydrogen isotopic ratios

576   of plant wax n-alkanes in a peat bog deposited in northeast China during the last 16 kyr. *Org.*

577   *Geochem.* **2009**, *40*, 671-677.

578   (64) Holoubek, I.; Caslavsky, J.; Korinek, P.; Kohoutek, J.; Staffova, K.; Hrdlieka, A.;

579   Pokorny, B.; Vancura, R.; Helesic, J. Project Tocoen. Fate of Selected Organic Compounds in

580   the Environment. Part XXVII. Main Sources, Emission Factors and Input of PAHs in Czech

581   Republic. *Polycyclic Aromatic Compd.* **1996**, *9:1-4,* 151-157.

582   (65) Plachá, D.; Raclavská, H.; Matýsek, D.; Rümmeli, M. H. The polycyclic aromatic

583   hydrocarbon concentrations in soils in the Region of Valasske Mezirici, the Czech Republic.

584   *Geochem. T.* **2009**, *10:12,* doi: 10.1186/1467-4866-10-12.

585   (66) Zhang, Y.; Tao, S. Global atmospheric emission inventory of polycyclic aromatic

586   hydrocarbons (PAHs) for 2004. *Atmos. Environ.* **2009**, *43*, 812-81.

587   (67) Bergmann, F. D.; Abu Laban, N. M. F. H.; Meyer, A. H.; Elsner, M.; Meckenstock, R. U.

588   Dual (C, H) isotope fractionation in anaerobic low molecular weight (poly)aromatic

589   hydrocarbon (PAH) degradation: Potential for field studies and mechanistic implications.

590   *Environ. Sci. Technol.* **2011***, 45,* 16, 6947-6953.

591   (68) *OTE, a.s. Czech electricity and gas market operator.* Website; http://www.ote-cr.cz/

602 **SUPPORTING INFORMATION AVAILABLE**

603 Table S1. Compilation of literature values for isotopic signatures of primary sources

604 Table S2. Individual PAH concentrations ($\mu g \cdot g^{-1}$ dry weight) in forest soils from Czech

605 Republic

606 Table S3. $\delta^{13}C$ values of PAHs in forest soils from Czech Republic

607 Table S4. $\Delta^{14}C$ values of PAHs in forest soils from Czech Republic

608 Table S5. $\delta^{2}H$ values of PAHs in forest soils from Czech Republic

609 Figure S1. Relation between the ratio BaA to BaA + CHRY and the $\delta^{13}C$ values of the

610 "chromatographic window": BaA + CHRY (Panel A) and the ratio BaP to BaP + BeP and the

611 $\delta^{13}C$ values of the "chromatographic window": BaP + BeP (Panel B)

612 Figure S2. GC/MS chromatograms depicting the different PAH traps from Sample #1 isolated

613 by pcGC

614   Supplemental Text S1. Experimental section

615   Supplemental Text S2. Calculation of the isotopic signatures (end members) for the primary

616   PAHs sources

617   Supplemental Text S3. MATLAB script for the Bayesian calculation

618   This information is available free of charge via the Internet at http://pubs.acs.org.

Table 1. PAH concentrations and average carbon (Δ^{14}C and δ^{13}C) and hydrogen (δ^2H) values of PAHs in forest soils

Sample ID	Site	Longitude	Latitude	Altitude (m a.s.l.[a])	ΣPAH[b] ($\mu g \cdot g^{-1}$ d.w.[c])	δ^2H (‰)	δ^{13}C (‰)	Δ^{14}C (‰)
#1	Krušné hory-Červená jáma	13° 27.702'	50° 33.804'	840	7.35	-225.8 ± 4.9	-24.18 ± 0.10	-911 ± 87
#2	Lužické hory-Jedlová	14° 33.035'	50° 51.939'	520	5.52	-116.6 ± 3.4	-24.04 ± 0.17	-897 ± 19
#3	Krkonoše-Pašerácký chodník	15° 45.933'	50° 44.416'	1320	2.61		-24.13 ± 0.14	
#4	Jeseníky-Jelení loučky	17° 15.544'	50° 8.867'	1120	2.49		-23.81 ± 0.20	
#5	Beskydy-Kykulka	18° 26.447'	49° 34.523'	930	9.11	-135.5 ± 23.9	-23.94 ± 0.09	-942 ± 24
#6	Javorníky-Kohútka	18° 12.756'	49° 17.713'	811	5.88	-108.6 ± 3.1	-24.04 ± 0.14	-905 ± 18
#7	Košetice	15° 05.476'	49° 34.231'	495	0.872	-99.3 ± 10.6	-24.13 ± 0.17	-819 ± 14
#8	Novohradské hory-Vysoká	14° 44.141'	48° 42.808'	971	3.81	-112.8 ± 3.1	-24.05 ± 0.26	-884 ± 17
#9	Šumava-Boubín	13° 49.018'	49° 0.026'	1120	0.532		-23.97 ± 0.22	
#10	Český les-Čerchov	12° 46.813'	49° 22.946'	985	4.80	-107.0 ± 3.8	-24.19 ± 0.22	-886 ± 14
				Average±stdev	4.30 ± 2.77	-129.4 ± 44	-24.05 ± 0.12	-892 ± 37

[a] above sea level

[b] sum of 14 PAHs: phenanthrene, anthracene, fluoranthene, pyrene, benz[a]anthracene, triphenylene, chrysene, benzo[b]fluoranthene, benzo[j]fluoranthene, benzo[k]fluoranthene, benzo[e]pyrene, benzo[a]pyrene, indeno[1,2,3-cd]pyrene, benzo[ghi]perylene

[c] dry weight

Table 2. Isotopic signatures (end members) for the primary PAHs sources[a]

Primary Source/ Isotope (mean±stdev, ‰)	$\delta^{13}C$	δ^2H	$\Delta^{14}C$
C3 plant combustion[b]	-28.7 ± 1.4	-94 ± 3	+137.5 ± 21.9
Liquid fossil fuel combustion[c]	-25.3 ± 1.6	-62 ± 7.3	-1000 ± 0
Coal pyrolysis at low temperature (~650 ºC)[d]	-23.2 ± 1.1	-129 ± 20.8	-1000 ± 0
Coal pyrolysis at high temperature (~900 ºC)[e]	-26.8 ± 1.3	-73.2 ± 4.0	-1000 ± 0

[a] See Table S1 and Text S2 with a literature compilation of isotopic signatures and calculation of the primary PAH sources end members, respectively

[b] $\delta^{13}C$ and δ^2H values for biomass were calculated as the average between PAH-specific and bulk signatures found in the literature. Three and one literature sources were used for $\delta^{13}C$ and δ^2H, respectively. $\Delta^{14}C$ for biomass was calculated assuming equal contributions of fresh biomass (+50‰) and wood (+225‰).

[c] $\delta^{13}C$ and δ^2H values were calculated assuming equal contributions from diesel and gasoline sources. Five and two literature sources were used for $\delta^{13}C$ and δ^2H, respectively.

[d] δ^2H and $\delta^{13}C$ values reported for bulk coal were used as δ^2H-PAH and $\delta^{13}C$-PAH signatures for coal combustion at low temperature assuming that the PAHs derived from carbonization processes at low temperatures have isotopic values similar to those of the parent coals. Seven and three literature sources were used for $\delta^{13}C$ and δ^2H, respectively.

[e] Four and one literature sources were used for $\delta^{13}C$ and δ^2H, respectively.

Table 3. Source contributions of liquid fossil fuel combustion, coal combustion at low and high temperature and biomass combustion for the ΣPAH_{14} in forest soils based on a four-source Bayesian Markov Chain Monte Carlo statistical mass-balance model (mean ± stdev)

Sample ID	$f_{\text{liquid fossil fuel}}$ (%)	$f_{\text{low T coal}}$ (%)	$f_{\text{high T coal}}$ (%)	f_{biomass} (%)	f_{coal} $(f_{\text{low T coal}} + f_{\text{high T coal}})$ (%)	f_{fossil} $(f_{\text{low T coal}} + f_{\text{high T coal}} + f_{\text{liquid fossil fuel}})$ (%)
#1				7.9		92.1
#2	15.4 ± 10.3	62.3 ± 10.4	13.2 ± 9.6	9.1 ± 0.2	75.6 ± 10.3	90.9 ± 17.5
#5	9.6 ± 7.3	75.2 ± 8.8	10.1 ± 7.6	5.1 ± 0.1	85.3 ± 7.3	94.9 ± 13.8
#6	17.4 ± 11.6	59.7 ± 11.2	14.5 ± 11.0	8.4 ± 0.2	74.2 ± 11.6	91.6 ± 19.5
#7	17.9 ± 12.3	53.1 ± 12.1	13.2 ± 10.6	15.9 ± 0.3	66.2 ± 12.5	84.1 ± 20.4
#8	15.3 ± 10.6	61.3 ± 10.5	13.2 ± 9.6	10.2 ± 0.2	74.5 ± 10.6	89.8 ± 17.7
#10	17.7 ± 11.9	56.7 ± 11.4	15.6 ± 11.0	10.0 ± 0.2	72.3 ± 11.9	90.0 ± 19.8
Average	**15.6 ± 3.1**	**61.4 ± 7.6**	**13.3 ± 1.8**	**9.5 ± 3.3**	**74.7 ± 6.2**	**90.2 ± 3.5**

FIGURE CAPTIONS

Figure 1. Map depicting bottom-up emission inventory of total 16 PAHs in 2007 (grid 0.1° x 0.1°)[35]. The sampling sites are indicated with white triangles.

Figure 2. Two-dimensional dual-isotope presentation of PAH in forest soils from sites #1 (circles), #5 (diamonds), #6 (triangles) and average of #2, #7, #8 and #10 (squares). Panel (**A**): δ^2H *versus* $\delta^{13}C$, where symbol colors are based on PAH molecular weight: *m/z* 178 (dark blue), *m/z* 202 (light blue), *m/z* 228 (green), *m/z* 252 (yellow and orange), *m/z* 276 (red); Panel (**B**): δ^2H *versus* $\Delta^{14}C$, where symbol colors are based on PAH concentrations. Isotopic signatures of primary sources of PAH are shown: biomass combustion (green), peat (light grey), liquid fossil fuel combustion (black), high temperature coal combustion ("high-T coal", brown) and low temperature coal combustion ("low-T coal", dark grey). Isotopic signatures on primary sources are based on reported literature values (Tables 2 and S1). Abbreviations: phenanthrene (PHEN), anthracene (ANTH), fluoranthene (FLU), pyrene (PYR), benz[a]anthracene (BaA), chrysene (CHRY), benzo[b]fluoranthene (BbF), benzo[j]fluoranthene (BjF), benzo[k]fluoranthene (BkF), benzo[e]pyrene (BeP), benzo[a]pyrene (BaP), indeno[1,2,3-cd]pyrene (IcdP), benzo[ghi]perylene (BghiP).

Figure 3. Probability density functions (pdf) of the relative source contribution of PAHs benzo[b+j+k]fluoranthene for Sample #7 (Panel **A**) and source contributions of fossil (liquid fuel + coal), liquid fossil fuel, coal combustion at low and high temperature and biomass combustion for the sum of PAHs in forest soils from Czech Republic (Panel **B**).

SOURCE APPORTIONMENT OF PAHs

Coal pyrolysis at high temperature (~900 ºC)?

Coal pyrolysis at low temperature (~650 ºC)?

ACS Paragon Plus Environment
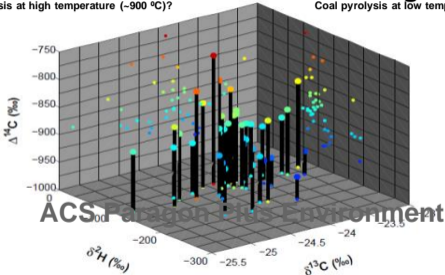
Liquid fossil fuel combustion?

Biomass combustion?
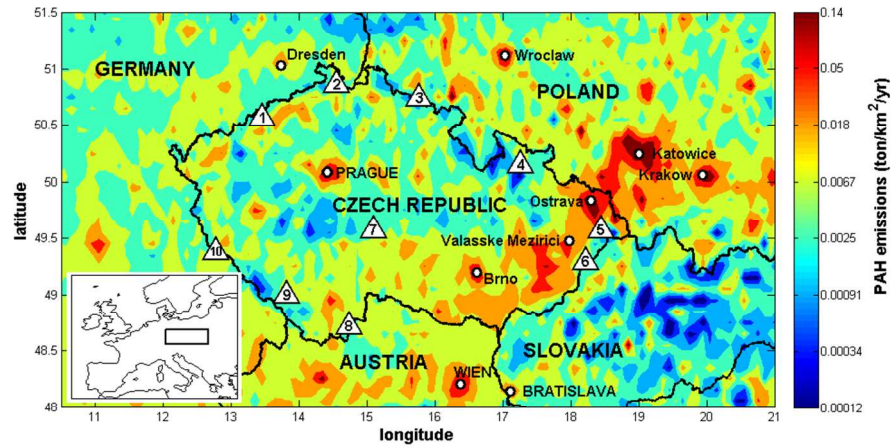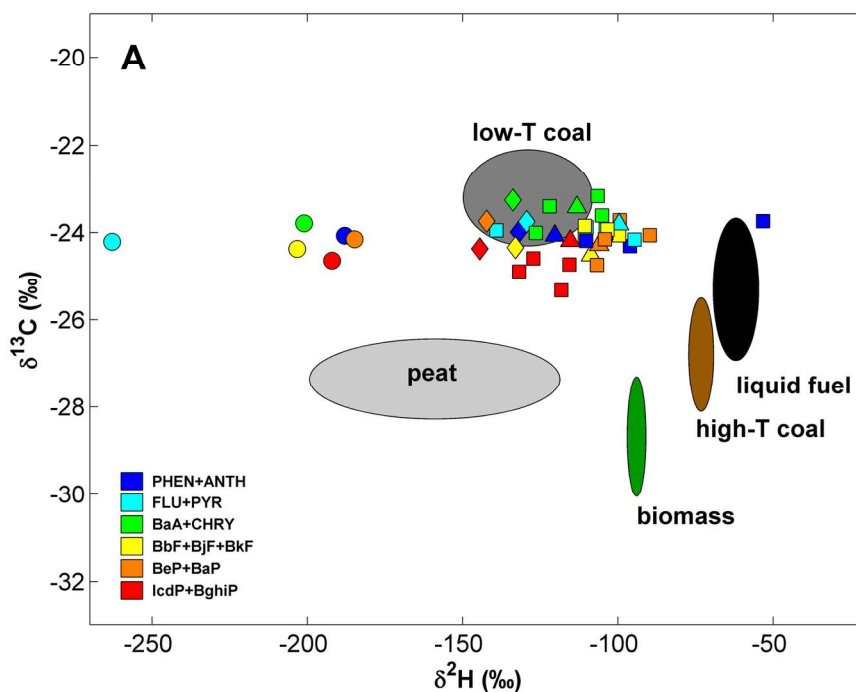
Figure 1. Map depicting bottom-up emission inventory of total 16 PAHs in 2007 (grid 0.1° x 0.1°)35. The sampling sites are indicated with white triangles.
292x164mm (96 x 96 DPI)

Figure 2. Two-dimensional dual-isotope presentation of PAH in forest soils from sites #1 (circles), #5 (diamonds), #6 (triangles) and average of #2, #7, #8 and #10 (squares). Panel (A): δ2H versus δ13C, where symbol colors are based on PAH molecular weight: m/z 178 (dark blue), m/z 202 (light blue), m/z 228 (green), m/z 252 (yellow and orange), m/z 276 (red); Panel (B): δ2H versus Δ14C, where symbol colors are based on PAH concentrations. Isotopic signatures of primary sources of PAH are shown: biomass combustion (green), peat (light grey), liquid fossil fuel combustion (black), high temperature coal combustion ("high-T coal", brown) and low temperature coal combustion ("low-T coal", dark grey). Isotopic signatures on primary sources are based on reported literature values (Tables 2 and S1). Abbreviations: phenanthrene (PHEN), anthracene (ANTH), fluoranthene (FLU), pyrene (PYR), benz[a]anthracene (BaA), chrysene (CHRY), benzo[b]fluoranthene (BbF), benzo[j]fluoranthene (BjF), benzo[k]fluoranthene (BkF), benzo[e]pyrene (BeP), benzo[a]pyrene (BaP), indeno[1,2,3-cd]pyrene (IcdP), benzo[ghi]perylene (BghiP). 152x114mm (300 x 300 DPI)
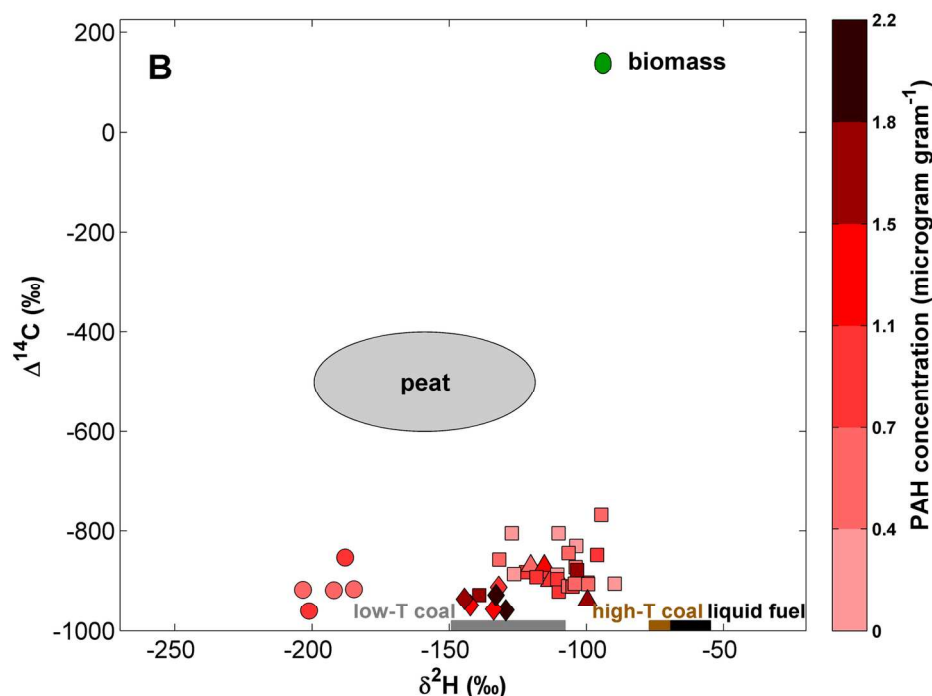
Figure 2. Two-dimensional dual-isotope presentation of PAH in forest soils from sites #1 (circles), #5 (diamonds), #6 (triangles) and average of #2, #7, #8 and #10 (squares). Panel (A): δ2H versus δ13C, where symbol colors are based on PAH molecular weight: m/z 178 (dark blue), m/z 202 (light blue), m/z 228 (green), m/z 252 (yellow and orange), m/z 276 (red); Panel (B): δ2H versus Δ14C, where symbol colors are based on PAH concentrations. Isotopic signatures of primary sources of PAH are shown: biomass combustion (green), peat (light grey), liquid fossil fuel combustion (black), high temperature coal combustion ("high-T coal", brown) and low temperature coal combustion ("low-T coal", dark grey). Isotopic signatures on primary sources are based on reported literature values (Tables 2 and S1). Abbreviations: phenanthrene (PHEN), anthracene (ANTH), fluoranthene (FLU), pyrene (PYR), benz[a]anthracene (BaA), chrysene (CHRY), benzo[b]fluoranthene (BbF), benzo[j]fluoranthene (BjF), benzo[k]fluoranthene (BkF), benzo[e]pyrene (BeP), benzo[a]pyrene (BaP), indeno[1,2,3-cd]pyrene (IcdP), benzo[ghi]perylene (BghiP). 152x114mm (300 x 300 DPI)
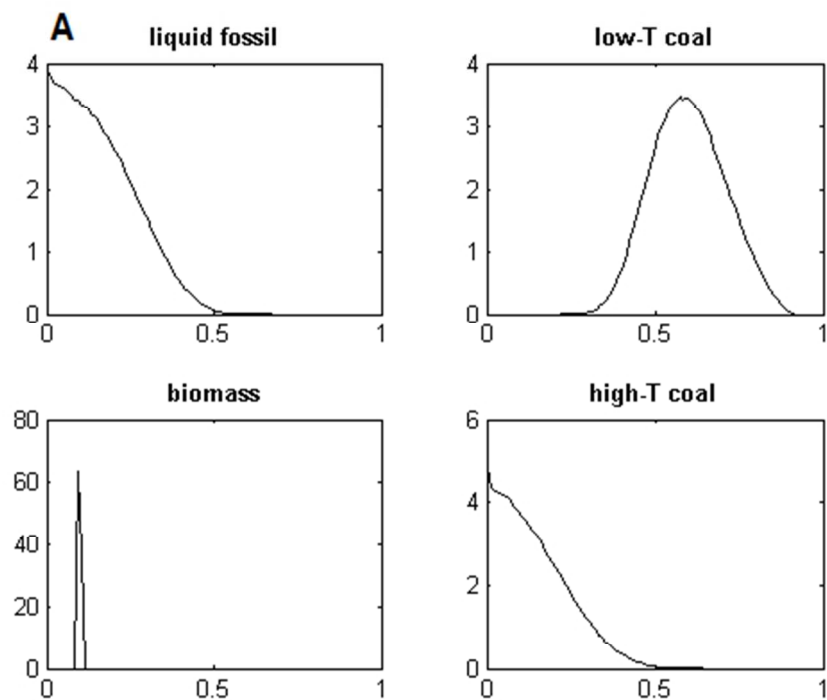
Figure 3. Probability density functions (pdf) of the relative source contribution of PAHs benzo[b+j+k]fluoranthene for Sample #7 (Panel A) and source contributions of fossil (liquid fuel + coal), liquid fossil fuel, coal combustion at low and high temperature and biomass combustion for the sum of PAHs in forest soils from Czech Republic (Panel B).
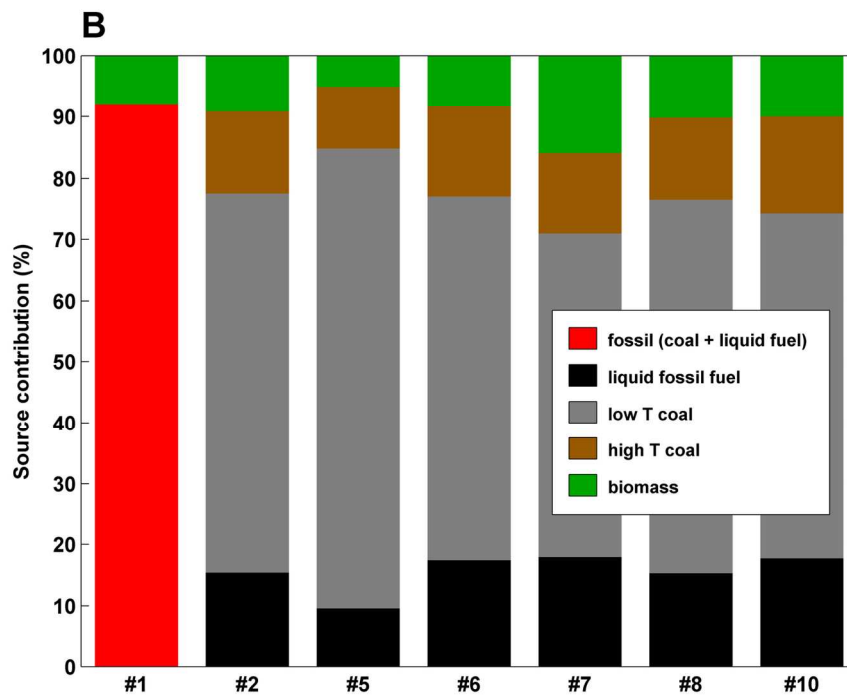148x111mm (96 x 96 DPI)

Figure 3. Probability density functions (pdf) of the relative source contribution of PAHs benzo[b+j+k]fluoranthene for Sample #7 (Panel A) and source contributions of fossil (liquid fuel + coal), liquid fossil fuel, coal combustion at low and high temperature and biomass combustion for the sum of PAHs in forest soils from Czech Republic (Panel B).
152x114mm (300 x 300 DPI)